

# Creating and distributing entanglement with spin chains

Irene D'Amico<sup>1,\*</sup> Brendon W. Lovett<sup>2,†</sup> and Timothy P. Spiller<sup>3,‡</sup>

<sup>1</sup> Department of Physics, University of York, York YO10 5DD, United Kingdom

<sup>2</sup> Department of Materials, University of Oxford, OX1 3PH, United Kingdom

<sup>3</sup> Hewlett-Packard Laboratories, Filton Road, Stoke Gifford, Bristol BS34 8QZ, United Kingdom

(Dated: February 9, 2020)

We show how branching spin chains can be used to both generate and distribute entanglement from their natural dynamics. Such entanglement provides a useful resource, for example for teleportation or distributed quantum processing. Once distributed, this resource can be isolated through mapping the entanglement into specific qubits at the ends of branches, or, as we demonstrate for distributed bipartite entanglement, applying simple single-qubit operations to the end spin of one or more branches.

PACS numbers: 03.67.Lx,03.67.-a,75.10.Pq,78.67.Hc,85.35.-p

## I. INTRODUCTION

Over the past few years there has been significant interest in the propagation of quantum information through spin chains. At a fundamental level, it is interesting to determine just what the natural dynamics of these systems permits. However, from a more practical quantum technology perspective, the controlled propagation of quantum information has potential use. For macroscopic distances, the current consensus is that photons, or other quantum states of light, form the best medium for quantum communication, as these can propagate through optical fibres or free space with high fidelity<sup>1</sup>. However, for much shorter, microscopic, distances it is possible that other media, such as spin chains, could make a very useful contribution. For example, in future solid state quantum information devices there could be a need to provide quantum communication links over microscopic distances, between separate quantum processors or registers, or between processors and memory, analogous to the conventional communication that goes on within the computer chips of today.

In this paper we use the terminology 'spin chain' to cover any physical system whose dynamics can be predicted using a Hamiltonian isomorphic to that of a coupled spin chain, which we shall define precisely later. In practice, this could be strings of actual spins (produced chemically, or fabricated) connected through interactions, or it could be a string of quantum dots or molecules (like fullerenes), containing exciton or spin qubits. Strings of trapped atoms form another possibility.

In order to quantify how well quantum processors or registers might communicate, there has been an emphasis on how well a quantum state can propagate through a spin chain or network. Originally it was shown that a single spin qubit could transfer with decent fidelity along a constant nearest-neighbour exchange-coupled chain<sup>2</sup>. The fidelity can approach unity if the qubit is encoded into a packet of spins<sup>3</sup>. Perfect state transfer can also be achieved in more complicated systems, with different geometry or chosen unequal couplings<sup>4,5,6,7</sup>. Parallel spins chains also enable perfect transfer<sup>8,9</sup>, as does a chain used as a wire, with controlled couplings at the ends<sup>10</sup>. Related studies have also been made on chains of quantum dots<sup>11</sup>, chains of quantum oscillators<sup>12,13</sup> and spin chains connected through long range magnetic dipole interactions<sup>14</sup>. State transfer and operations

through spin chains using adiabatic dark passage has also been proposed<sup>15,16</sup>.

In this work, we consider a different approach to the problem of short distance quantum communication. Rather than focus on spin chains providing high fidelity transfer of quantum information, our approach is to construct spin chain systems whose natural dynamics creates high fidelity spatially separated entanglement from a simple initial state. The creation of such separated entanglement<sup>15,17,18,19</sup> provides a useful and flexible quantum information resource. For example, it could be used for quantum teleportation<sup>20</sup>, which enables the transfer of a quantum state, or to connect separated quantum registers or processors. One advantage of this approach is that decoherence or imperfections, which can lead to imperfect entanglement production, could be countered by purification techniques<sup>21</sup> prior to use of the entangled resource. We will use a spin chain formalism common to most of the cited works.

## II. SPIN CHAIN FORMALISM

To introduce our formalism, we first consider a one-dimensional chain of  $N$  spins, each coupled to their nearest neighbours. The Hamiltonian for the system is

$$H = - \sum_{i=1}^N \frac{E_i}{2} \sigma_z^i + \sum_{i=1}^{N-1} \frac{J_{i,i+1}}{2} (\sigma_+^i \sigma_-^{i+1} + \sigma_-^i \sigma_+^{i+1}), \quad (1)$$

where  $\sigma_z^i$  is the  $z$  Pauli spin matrix for the spin at site  $i$  and similarly  $\sigma_{\pm}^i = \sigma_x^i \pm i\sigma_y^i$ . For actual spins,  $E_i/2$  is the local magnetic field (in the  $z$ -direction) at site  $i$  and  $J_{i,i+1}/2$  is the local  $XY$  coupling strength between neighbouring sites  $i$  and  $i+1$ . For a coupled chain of quantum dots where each qubit is represented by the presence or absence of a ground state exciton,  $E_i$  is the exciton energy and  $J_{i,i+1}$  is the Förster coupling between dots  $i$  and  $i+1$ <sup>11</sup>. The spin chain formalism applies to both such physical systems, and to any others which can be described by an isomorphic Hamiltonian. The computational

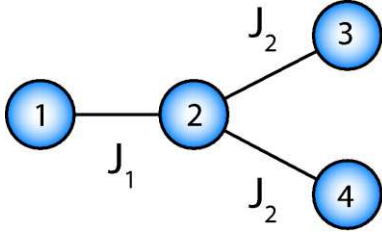


FIG. 1: A schematic four-site Y spin chain system, with nearest neighbour couplings as shown.

basis notation for the spin states at each site is  $|0\rangle_i \equiv |\uparrow_z\rangle_i$  and  $|1\rangle_i \equiv |\downarrow_z\rangle_i$ .

The total  $z$ -component of spin (magnetisation), or total exciton number, is a constant of motion as it commutes with  $H$ . It is therefore instructive to consider a state of the system consisting of the ground state with the addition of a single flipped spin. This state is straightforward to prepare, assuming local control over a spin at, say, the end of a chain, and the flipped spin can be regarded as a (conserved) travelling qubit as it moves around under the action of the chain dynamics<sup>2</sup>. An efficient way of representing such states in an  $N$  spin network is the site basis defined as  $|\mathbf{k}\rangle = |0_1, 0_2, \dots, 0_{k-1}, 1_k, 0_{k+1}, \dots, 0_N\rangle$ . A system prepared in this subspace remains in it. Now the detailed dynamics depend on the local magnetic fields or exciton energies, but if these are independent of location  $i$  then the dynamics favour quantum state transfer processes, as already mentioned. We also adopt this limit for our work here.

### III. BI-PARTITE ENTANGLEMENT CREATION AND DISTRIBUTION

Rather than using spin chains to transfer quantum states, our focus here is to use spin chain systems to prepare spatially separated entanglement, which can then be used as a resource for teleportation, or providing quantum connections between separated quantum processors or registers. The simplest system we consider is a Y structure, chosen to prepare bi-partite entanglement from a simple initial state. The smallest definable Y structure contains four sites, which we label as shown in Fig. 1.

As seen in the figure, there is a deliberate asymmetry in the coupling of the outside sites to the hub of the Y. There is one ‘‘input’’ site, coupled to the hub with strength  $J_1$ , and two ‘‘output’’ sites, coupled to the hub with equal strength  $J_2$ . The Hamiltonian for this system is written:

$$H_{Y4} = J_1 |1\rangle\langle 2| + J_2 (|2\rangle\langle 3| + |2\rangle\langle 4|) + H.c.. \quad (2)$$

We proceed by noting that  $|-\rangle \equiv 2^{-\frac{1}{2}}(|3\rangle - |4\rangle)$  is an eigenstate of the system. If we initialise our system in the state  $|1\rangle$  then  $|-\rangle$  is decoupled and plays no part in our system dynamics. We define the orthogonal state  $|+\rangle \equiv 2^{-\frac{1}{2}}(|3\rangle + |4\rangle)$  and

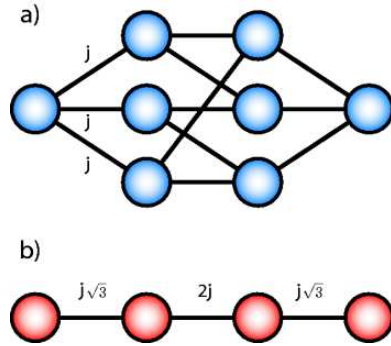


FIG. 2: (a) Example of a qubit network. All the couplings are equal and have strength  $j$ . (b) Equivalent one-dimensional chain with unequal couplings.

rewrite our Hamiltonian in the  $\{|1\rangle, |2\rangle, |+\rangle\}$  space as:

$$H'_{Y4} = J_1 |1\rangle\langle 2| + J_2\sqrt{2} |2\rangle\langle +| + H.c. \quad (3)$$

This shows that our system is equivalent to a 1D three-site spin chain where the ‘‘output’’ site is the symmetric entangled state  $(|0\rangle_3|1\rangle_4 + |1\rangle_3|0\rangle_4)$ . Such a chain effects perfect state transfer from the input site 1 to the entangled output so long as the couplings are equal – i.e. if  $J_1 = J_2\sqrt{2}$ .

In the following we will show that we can extend this entanglement creation and distribution to spin chain systems with longer arms. To do this using the approach introduced above is rather cumbersome. Rather, we shall use the method of analysis introduced by Christandl *et al.* in Ref. 5. They find that perfect transfer along a longer chain is possible through the use of  $N - 1$  unequal couplings along an  $N$  site chain, which satisfy

$$J_{i,i+1} = \alpha\sqrt{i(N-i)}. \quad (4)$$

where  $\alpha$  is a constant that sets the size of the interaction and  $J_{i,i+1}$  is the coupling between site  $i$  and site  $i + 1$ . The authors of Ref. 5 also show that an array of spins with equal couplings  $j$  can be projected onto a 1D chain of unequal couplings. In particular, consider an array that is arranged as a series of columns. Let each node of column  $i$  be connected to  $n$  different nodes of adjacent column  $i + 1$ , and each node of column  $i + 1$  be connected to  $m$  different nodes of column  $i$ . Christandl *et al.* then show that each column can be projected onto a single node of a one dimensional spin chain with coupling  $j\sqrt{mn}$  between nodes  $i$  and  $i + 1$ . An example is shown in Fig. 2.

If we analyse the four site Y-chain of Fig. 1 in this way, it is trivial to see that the Y-chain is equivalent to a 1D chain with couplings  $J_1, J_2\sqrt{2}$ , exactly as before. According to the general properties of a 3-node chain<sup>5</sup>, this structure allows for perfect transfer between the two extremes so long as  $J_1 = J_2\sqrt{2}$ . In this case, the perfect transfer of an excitation in node 1 is allowed across the Y-shaped structure to the sites at the extremes 3 and 4, where it must be shared between the two ends, giving rise to entanglement.

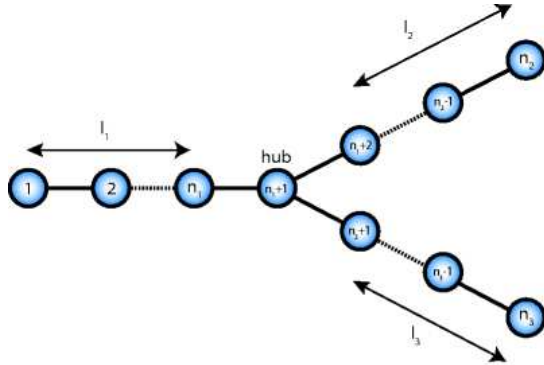


FIG. 3: Relevant notation for ‘star’ structures.

We can extend this kind of analysis to larger structures, and we now introduce a labelling convention to deal with these. Referring to Fig. 3, we choose to number branches clockwise, starting from the input chain. The length of branch  $k$  (excluding the hub) is indicated as  $l_k$ . A Y-structure is then specified by the sequence of numbers  $(l_1, l_2, l_3)$ . Integer labels  $i$  will be used for each of the total  $N$  sites in the structure as follows: Starting with site  $i = 1$  at the left-most site of the input chain, label in sequence up to and including the hub. Continue by labelling along output branch 2, to its end, and then continue further by labelling branch 3, starting from the site adjacent to the hub and going to its end. If the site furthest from the hub of branch  $k$  is called  $n_k$  then  $n_1 = 1$ ,  $n_2 = l_1 + l_2 + 1$  and  $n_3 = N = l_1 + l_2 + l_3 + 1$ .

To demonstrate the generation and perfect transfer of bipartite entanglement to the output spins  $n_2$  and  $n_3$ , we have performed dynamical simulations using the Hamiltonian of Eq. (1), the condition Eq. (4) and the branching rule for the couplings at the hub spin. Fig. 4 shows how the hub branching rules applies to the  $(3, 3, 3)$  structure, where  $J_1 = J_6 = \alpha\sqrt{6}$ ,  $J_2 = J_5 = \alpha\sqrt{10}$ ,  $J_3 = \alpha\sqrt{12}$ ,  $J_4 = \alpha\sqrt{6}$  for perfect state transfer. Fig. 5 shows the result of the simulations for both the  $(3, 3, 3)$ ,  $N = 10$ , and  $(10, 10, 10)$ ,  $N = 31$ , structures. The initial condition is  $c_1 = 1$  (and all others zero), where  $c_i$  indicates the amplitude coefficient for the state  $|i\rangle$ . The upper panel of Fig. 5 shows the temporal evolution of  $|c_1|^2$  and  $|c_N|^2$  for the two systems. We underline that, due to symmetry, spins  $N (= n_3)$  and  $n_2$  have the same dynamics in this case, and our results show that the excitation is completely transferred from site 1 to sites  $n_2$  and  $n_3$  at time  $\pi/2\alpha$  and periodically returns there at regular time intervals of  $\pi/\alpha$ . In respect to the rescaled time  $\alpha t$ , the peak corresponding to each revival narrows as the length  $l_k$  of the branches increases. This is important when considering an optimal practical structure for distributing entanglement, since a narrower peak puts greater time constraints on any entanglement extraction protocol. The lower panel of Fig. 5 shows the corresponding fidelity with respect to the state  $|+\rangle \equiv 2^{-\frac{1}{2}}(|n_2\rangle + |n_3\rangle)$ .

We can quantify the amount of entanglement at the chain ends (as a function of time) more formally by using the entanglement of formation,  $E_F$ . This has a value unity for a maximally entangled state and zero for an unentangled one. Specifically, it measures the number of Bell states required to

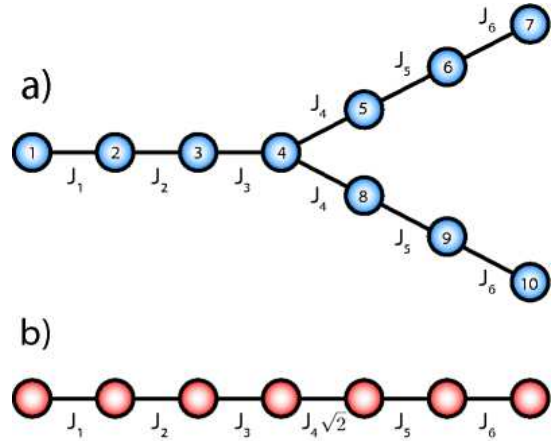
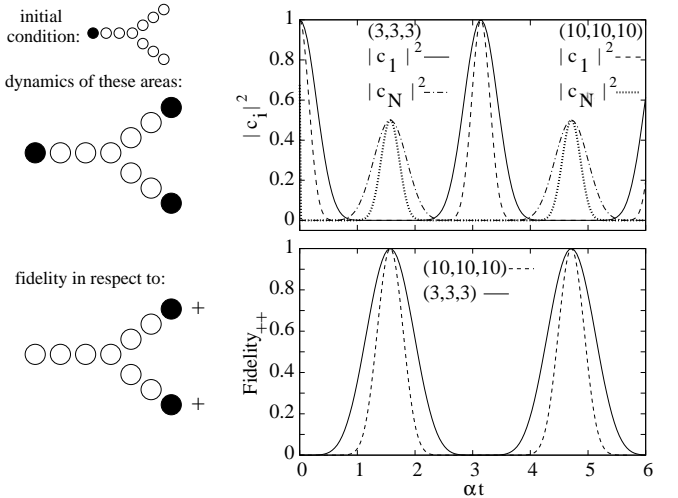


FIG. 4: (a) Ten site Y spin chain network. Its equivalent one-dimensional representation is shown in (b).

FIG. 5: Results of simulations on a  $(3,3,3)$  and a  $(10,10,10)$  Y spin chain system, with nearest neighbour couplings chosen to satisfy Eq. (4) and the hub branching rule. Initial condition:  $c_1 = 1$ . Upper panel:  $|c_1|^2$  and  $|c_N|^2$  with respect to the rescaled time  $\alpha t$ . Lower panel: corresponding fidelity with respect to the state  $|+\rangle \equiv 2^{-\frac{1}{2}}(|n_2\rangle + |n_3\rangle)$ .

create the state of interest and for a two qubit state it is given by:

$$E_F(\rho) = h\left(\frac{1 + \sqrt{1 - \tau}}{2}\right), \quad (5)$$

where  $h(x) = -x \log_2(x) - (1-x) \log_2(1-x)$  is the Shannon entropy function.  $\tau$  is the “tangle” or “concurrence” squared:

$$\tau = C^2 = [\max\{\lambda_1 - \lambda_2 - \lambda_3 - \lambda_4, 0\}]^2. \quad (6)$$

The  $\lambda$ ’s are the square roots of the eigenvalues, in decreasing order, of the matrix  $\rho\tilde{\rho} = \rho \sigma_y^A \otimes \sigma_y^B \rho^* \sigma_y^A \otimes \sigma_y^B$ , where  $\rho^*$  denotes the complex conjugation of  $\rho$  in the computational basis  $|00\rangle, |01\rangle, |10\rangle, |11\rangle$ <sup>22</sup>.

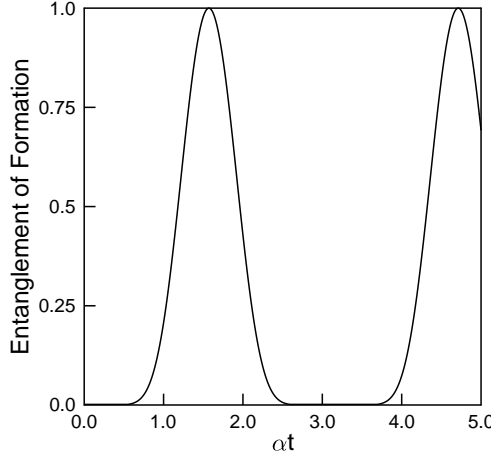


FIG. 6: Entanglement of Formation of the two chain end qubits ( $n_2 = 7$  and  $n_3 = 10$ ) of the ten site Y chain shown in Fig. 4, following the initialisation procedure described in the text.

$E_F$  between qubits  $n_2 = 7$  and  $n_3 = 10$  of the (3, 3, 3) structure is shown in Fig. 6, as a function of time following initialisation of the excitation on site 1. As would be expected, a maximally entangled state is obtained after a time  $\pi/2\alpha$  and at intervals of  $\pi/\alpha$  thereafter.

Maximally entangled states can be produced even if the length of the output branches,  $l_2 = l_3$ , is different from the length of the input branch  $l_1$ , as long as the nearest neighbour couplings satisfy Eq. (4) and the hub branching rule. As an example in Fig. 7 we compare the results for the systems (3, 3, 3), (5, 2, 2) and (7, 1, 1), with notation and initial condition as in Fig. 5. Our results show the perfect generation of an output entangled state, as before, at time  $t = \pi/2\alpha$  from a simple initial input excitation even for the more asymmetric systems. As the asymmetry increases, the width of the peaks decreases, but the change is not significant.

#### IV. GENERALISATION TO $p$ OUTPUTS

The branching rule we have given for preparation of bipartite entanglement using a Y spin chain structure can be extended to the case of the different families of tree-like spin chain structures with a single input and  $n$  output branches. Examples of their members are represented in Fig. 8.

Panel (a) corresponds to a ‘star-like’ family, in which there is just one hub and all output branches have the same length. Extending the notation early introduced, we can indicate the members of this family as  $(m, l, l, l, \dots, l)$ . Following on from the arguments in Section III, the coupling on the outputs from the hub spin are all reduced by a factor of  $1/\sqrt{p}$  compared to the effective one-dimensional spin chain value. The entangled state which can be created by using this family is a W-state, consisting of an excitation shared between  $p$  separated sites, with the *symmetric* form  $(|1_{n_2}, 0_{n_3}, \dots, 0_{n_p}\rangle + |0_{n_2}, 1_{n_3}, \dots, 0_{n_p}\rangle + \dots + |0_{n_2}, 0_{n_3}, \dots, 1_{n_p}\rangle)/\sqrt{p}$ . In real sys-

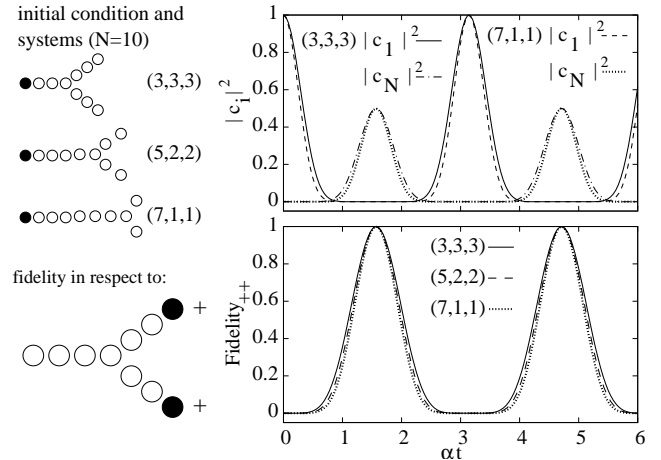


FIG. 7: Results of simulations on a (3, 3, 3), (5, 2, 2) and (7, 1, 1) Y spin chain system, with nearest neighbour couplings chosen to satisfy Eq. (4) and the hub branching rule. Initial condition:  $c_1 = 1$  Upper panel:  $|c_1|^2$  and  $|c_N|^2$  as a function of the rescaled time  $at$ . Lower panel: corresponding fidelity with respect to the state  $|+\rangle \equiv 2^{-\frac{1}{2}}(|n_2\rangle + |n_3\rangle)$

tems it is likely to be impractical to prepare  $p$ -way entangled states using this approach for large values of  $p$ . However, if three-dimensional physical structures can be built—and for example there is the potential for this with quantum dot systems—modest values of  $p > 2$ , such as 3, 4 and 5 could be possible.

Panel (b) gives an example of what we refer to as a bifurcation-like structure. These structures contain more than one hub—and for perfect transfer the branching rule must be implemented at each. Note that for timing of the dynamical evolution to produce complete excitation transfer to the outlying sites, the number of sites along all output paths from the initial hub must be the same. The entangled states which can be created by using this family share the excitation between the different separated outlying sites with different unequal weights. e.g. the structure represented in panel (b) gives the form  $|1_{n_2}, 0_{n_3}, 0_{n_4}\rangle/\sqrt{2} + |0_{n_2}, 1_{n_3}, 0_{n_4}\rangle/2 + |0_{n_2}, 0_{n_3}, 1_{n_4}\rangle/2$ . With only modest branching at each hub, a bifurcating structure potentially could be fabricated in a planar arrangement. This could in principle give rise to a significant number of output branches, whose outlying spins can be entangled, sharing an excitation in an *asymmetric* manner, where the type of asymmetry depends on the number of hubs and on their position.

#### V. EXTRACTION OF ENTANGLEMENT

Having generated and distributed, for example, bi-partite entanglement using a Y spin chain system, it is useful to be able to isolate this entanglement in some way, so it can be used as a resource. Clearly, as illustrated in figure 6, the arrival time of the entangled state at the output relative to the preparation time of the excitation at the input is known. However, if the entanglement is being created as a resource (and

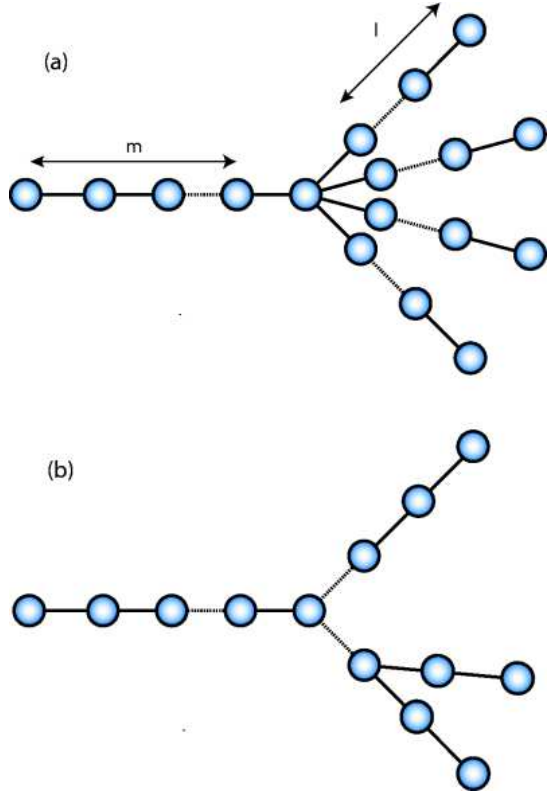


FIG. 8: (a) Example of a star-like family member  $(m, l, l, l, l)$ . (b) Example of a bifurcation-like family member.

particularly if a number of such states are to be purified before use) then it is essential to preserve it once it is created. This might be done by extracting it (e.g. with swap operations) from the spin chain system and transferring it to a storage system of qubits, or to members of spatially separated quantum registers or processors. See Ref. 19 for a method of doing this with an excitonic quantum dot system. Certainly such swapping is likely to be necessary in any excitonic realisation of a spin chain, if the entangled resource is required to exist on timescales longer than the ground state exciton coherence times and lifetimes<sup>19</sup>. Another possibility is to physically isolate the two nodes at the end of the chain, after the entanglement has formed there. If fast local control of the couplings is possible, then the state could indeed be frozen at the ends of the output branches. To achieve this the couplings have to be switched fast on a timescale set by the chain dynamics, as illustrated by Fig. 6, and this has to be done simultaneously on both output branches. In general both the freezing of the spatially separated entanglement, and its swapping into longer-lived “memory” qubits at the ends of the output branches of the spin chain systems, requires fast, coordinated action at the ends of both branches. This may be fine if these actions are both controlled through external optical pulses.

However, there is another approach to preserving the entanglement, which could be very effective for some realisations of the spin chain systems. This can be implemented when an entangled state is (a) an eigenstate of the Hamiltonian Eq. (1)

and (b) it can be reached with just *one* single qubit local operation from the entangled state provided by the natural dynamics of the system. In this case isolation of the entanglement requires just a single fast single-qubit operation at one of the two branch ends. The simplest example of this is again with the four-site system illustrated in Fig. 1. As already remarked, the antisymmetric entangled state  $|-\rangle \equiv 2^{-\frac{1}{2}}(|3\rangle - |4\rangle)$  is an eigenstate of the system, decoupled from the transfer dynamics (The state of qubits 3 and 4 for a system in the  $|-\rangle$  state, after tracing out the others, is the maximally entangled  $2^{-\frac{1}{2}}(|0\rangle_3|1\rangle_4 - |1\rangle_3|0\rangle_4)$ ). After state transfer, our system is in the  $|+\rangle$  state defined earlier. If a phase flip gate, for example  $|0\rangle \rightarrow |0\rangle$  and  $|1\rangle \rightarrow -|1\rangle$ , fast on the timescale of the spin chain dynamics, is applied to just one chain end qubit (3 or 4) of the  $|+\rangle$  state, we obtain  $|-\rangle$ . Thus our entangled resource can be frozen into an eigenstate of this four-site system.

Things are not quite so simple in larger Y spin chain systems. If a phase flip is applied to the output entangled state of a larger Y spin chain system, this opposite parity entangled state is not an eigenstate of the full system. However, the entanglement is effectively “dynamically frozen” by the action of the single-qubit phase flip, in the sense that the subsequent dynamics just involves the spins in  $l_2$  and  $l_3$  and the  $|-\rangle$  entangled state between spins  $n_2, n_3$  revives periodically and more frequently than if the phase flip is not applied. This is illustrated in Fig. 9 for the systems  $(3, 3, 3)$ ,  $(5, 2, 2)$  and  $(7, 1, 1)$ , where the results of simulations are presented for the initial condition  $|-\rangle \equiv 2^{-\frac{1}{2}}(|n_2\rangle - |n_3\rangle)$ . Couplings are chosen to satisfy Eq. (4) and the hub branching rule. The upper panel shows the fidelity with respect to the state  $|-\rangle$  (‘Fidelity<sub>+</sub>’). These results show the perfect revival of an output entangled state with a period shorter than  $\pi/\alpha$ . For the system  $(3, 3, 3)$ , comparison between Fig. 7 and Fig. 9 shows that the revival spacing is  $\pi/2\alpha$  in this case. As the dynamics of the system is restricted by quantum destructive interference to the spins in  $l_2$  and  $l_3$ , the time of revival decreases with decreasing  $l_2 = l_3$ . For the limit case  $(7, 1, 1)$  – in which  $l_2 = l_3 = 1$  – the state  $|-\rangle$  is again an eigenstate of the system, so that the entangled state is frozen at the output spins  $n_2$  and  $n_3$ . This suggests that a system represented by  $(m, 1, 1)$  could be used to create entanglement in two qubits on a distant ( $m$  spins away) array or register. In this case the entanglement could then be trapped in the two qubits by a single qubit operation applied to one of them. This system could also be used as a switch, for example to start a computation, or to initialise from a distance the creation of entangled states needed for measurement-based computation<sup>17</sup>. The middle panel shows the dynamics of  $|c_i|^2$  for the spins in  $l_3$  plus the hub spin for  $(3, 3, 3)$ . Clearly the hub is never involved in the dynamics (the line labelled as ‘a’). The lines labelled from ‘b’ to ‘d’ correspond to the dynamics of spins in  $l_3$  from the hub outward. No spin in  $l_1$  is involved in the dynamics (not shown). This can be understood from initial condition, in which the dynamics of the two output branches is out of phase by  $\pi$ . The symmetry of the structure and of the bonds must therefore generate *destructive* interference in  $l_1$  and the hub. The lower panel shows the corresponding dynamics for the  $(5, 2, 2)$  system. Note that, since in this case  $l_2 = l_3 = 2$ , the dynamics oscillates perfectly

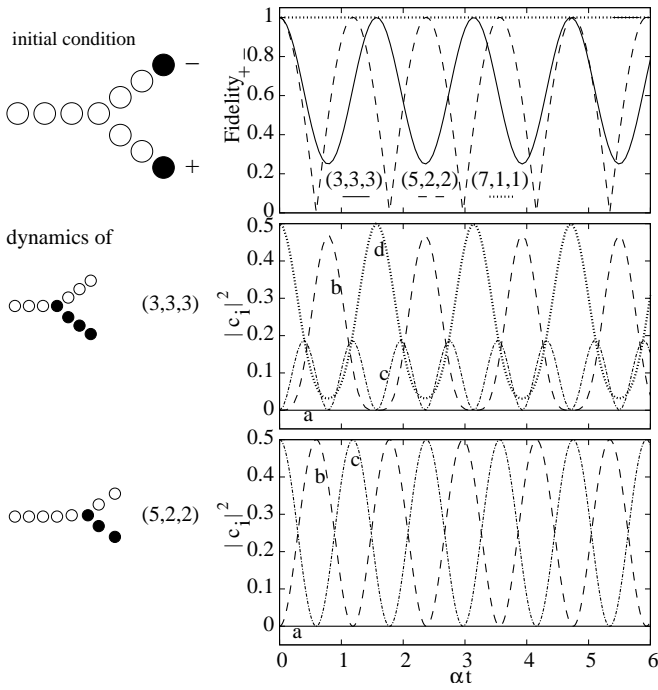


FIG. 9: Simulations on a  $(3, 3, 3)$ ,  $(5, 2, 2)$  and  $(7, 1, 1)$  Y spin chain system, with nearest neighbour couplings chosen to satisfy Eq. (4) and the hub branching rule. Initial condition:  $|-\rangle \equiv 2^{-\frac{1}{2}}(|n_2\rangle - |n_3\rangle)$ . Upper panel: Fidelity with respect to the state  $|-\rangle$  as a function of the rescaled time  $\alpha t$ . Middle panel:  $|c_i|^2$  for the spins in  $l_3$  plus the hub spin for  $(3,3,3)$ . The line labelled as ‘a’ represents the hub dynamics; ‘b’ to ‘d’ represent the dynamics of spins in  $l_3$  from the closest to the hub (b) to  $n_3$  (d). Lower panel:  $|c_i|^2$  for spins in  $l_3$  plus the hub for  $(5,2,2)$ . The line labelled as ‘a’ represents the hub dynamics, ‘b’ the dynamics of the spin closest to the hub and ‘c’ the dynamics of  $n_3$ .

between the spins  $\{n_2, n_3\}$  and their *respective* nearest neighbours  $\{n_2-1, n_3-1\}$ . Fig. 10 shows the detailed dynamics of the components of  $c_i$  for  $\{n_2, n_3\}$  (upper panel, where the coefficient is purely real) and  $\{n_2-1, n_3-1\}$  (lower panel, where the coefficient is purely imaginary). A (maximally) entangled state of the type  $|-\rangle$  is periodically and perfectly transferred between the two pairs of spins. For the general  $(x, 2, 2)$  system with this initial condition, the dynamics oscillate between two maximally entangled states, which have a phase difference.

As pointed out above, the destructive interference at the hub and in branch  $l_1$  is caused by (i) the antisymmetric initial condition of the type  $|-\rangle$ , (ii) the symmetry of the systems, i.e.  $l_2 = l_3$  and (iii) the same sequence of bonds in  $l_2$  and  $l_3$ . What is more interesting is that this is a *sufficient* condition to ensure perfect periodic revival of entanglement at the output spins. This can be understood by defining an operator  $S$ , which swaps the two outgoing branches of any Y structure. Clearly  $|+\rangle$  ( $|-\rangle$ ) is an eigenstate of  $S$  with eigenvalue  $+1$  ( $-1$ ) and, further,  $S$  commutes with any Hamiltonian that has equivalent outgoing branches. We underline that these need not satisfy any special coupling rule, only the condition that the two branches have to be the same.  $S$  is thus conserved and

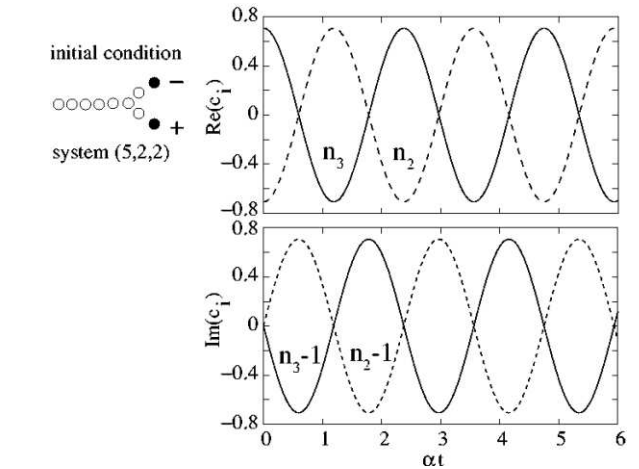


FIG. 10: Results of simulations on a  $(5, 2, 2)$  Y spin chain system, with nearest neighbour couplings chosen to satisfy Eq. (4) and the hub branching rule. Initial condition:  $c_{n_3} = -c_{n_2} = 1/\sqrt{2}$ . Dynamics of real part of  $c_{n_2}$  and  $c_{n_3}$  (Upper panel) and imaginary part of  $c_{n_2-1}$  and  $c_{n_3-1}$  (Lower panel).

so any state with eigenvalue  $-1$  must always have zero amplitude at the hub and in the input branch. For a finite Y system, an initial state of  $|-\rangle$  will therefore always revive, with the hub and input branch having zero amplitude at all times. This can be illustrated in numerical examples. In Fig. 11 we present the results of simulations on a  $(3, 3, 3)$  spin chain, for two systems in which the set of nearest neighbour couplings is generated using a flat distribution in the interval  $(0, 1]$ , but satisfying the condition that bonds in  $l_2$  and  $l_3$  (including the one to the hub) have the same sequence. The initial condition is given by  $|-\rangle \equiv 2^{-\frac{1}{2}}(|n_2\rangle - |n_3\rangle)$ . The upper panel shows the fidelity with respect to the state  $|-\rangle$  for two choices of random couplings: A (solid line) and B (dashed-dot line) as a function of the rescaled time  $\alpha t$ . As can be seen, the fidelity pattern is more complicated than for the case of coupling following the prescription given by Eq (4) and the hub branching rule. In particular peaks are present which do not correspond to maximum fidelity. Nevertheless peaks corresponding to fidelity of unity appear periodically, with the period determined by the particular sequence of bonds. The middle (lower) panel shows the dynamics of  $|c_i|^2$  for spins in  $l_3$  and the hub for system A (B). We remark that neither system A nor B allows for perfect transfer between spin 1 and spins  $\{n_2, n_3\}$ : the condition for perfect transfer is a more delicate one and in particular does not rely on simple symmetry considerations.

Rather than simply dynamically freezing entanglement by shortening its revival time, a combination of the entanglement extraction ideas can be used to actually freeze spatially separated entanglement in systems of the bifurcation family. For example, consider a Y structure where at the end of each output branch there is a bifurcation into two final spins. This is illustrated in Fig. 12. In terms of the four end spins, the natural dynamics will generate a state of the form  $\frac{1}{2}(|0, 0, 0, 1\rangle + |0, 0, 1, 0\rangle + |0, 1, 0, 0\rangle + |1, 0, 0, 0\rangle)$ . This is shown in Fig. 12 by plotting the branch end spin probabilities

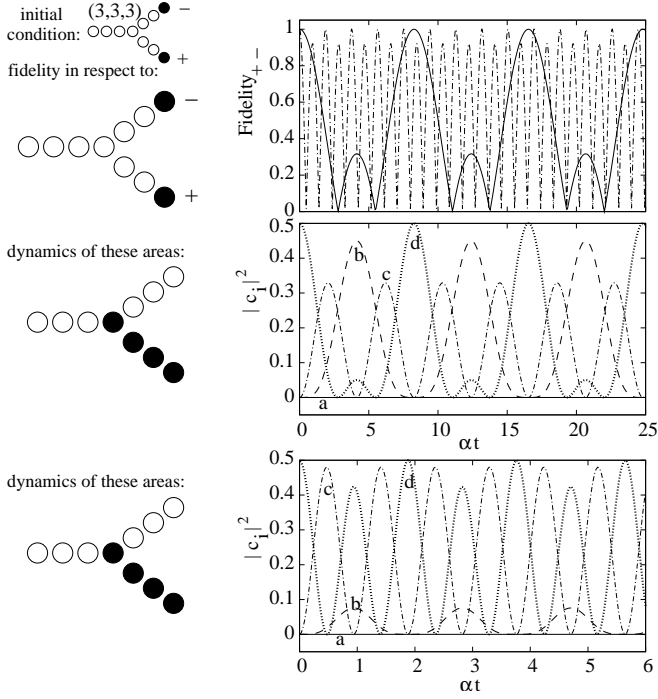


FIG. 11: Results of simulations of  $(3, 3, 3)$  Y spin chain systems with nearest neighbour couplings generated using a flat distribution over  $(0,1]$ , but satisfying the condition that the bonds in  $l_2$  and  $l_3$  (and to the hub) have the same sequence. Initial condition  $|-\rangle \equiv 2^{-\frac{1}{2}}(|n_2\rangle - |n_3\rangle)$ . Upper panel: Fidelity with respect to the state  $|-\rangle$ . Middle panel:  $|c_i|^2$  versus the rescaled time  $\alpha t$  for spins in  $l_3$  plus the hub for the random set of couplings A (solid line in upper panel). The line labelled as ‘a’ represents the hub dynamics, and ‘b’ to ‘d’ the dynamics of spins in  $l_3$  from the closest to the hub (b) to  $n_3$  (d). Lower panel: As for the middle panel but for random set B (dashed-dot line in upper panel). Note the different scale on the time axis here.

$|c_{n_i}|^2$  as a function of rescaled time  $\alpha t$ . If at a probability peak a phase flip is applied to one spin out of each pair, a state of the form  $\frac{1}{2}(|0,0,0,1\rangle - |0,0,1,0\rangle + |0,1,0,0\rangle - |1,0,0,0\rangle)$  results. This is an eigenstate of the system and the entanglement is thus frozen. Although four spins are involved, the spatial separation achieved is between two pairs of spins, so the pairs could each be viewed as storage buffers for one qubit. In this sense the system contains *spatially separated and stored bipartite entanglement*, which could be released for future use by single qubit operations and/or coupling to other systems at the branch ends.

## VI. CONCLUSIONS

We have shown how branching spin chain systems can be used to both generate and distribute entanglement from their natural dynamics. Once distributed, this entanglement can be isolated through mapping the entanglement into specific qubits at the ends of branches, or, as we have shown for distributed bipartite entanglement, applying a simple single-qubit operation to one end spin of a branch. Given its simplic-

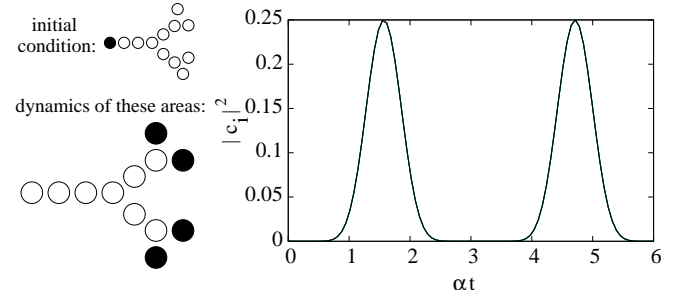


FIG. 12: Dynamics of  $|c_{n_i}|^2$  (for the output branch end spins) versus the rescaled time  $\alpha t$ , for the bifurcation structure shown. This follows the initialisation condition  $c_1 = 1$ .

ity, this latter approach may be particularly useful in initial experimental investigations of such branched systems.

Distributed entanglement provides a useful resource, for example for teleportation<sup>20</sup> or distributed quantum processing. In contrast to the use of spin chains to propagate quantum states from one place to another with as high a fidelity as possible, there could be some advantage in building up a high fidelity entangled resource “off line”. Real systems, with their inevitable imperfections, will almost certainly degrade transmission fidelities, even if in principle these approach unity. Certainly, with the “off line” resource approach, purification<sup>21</sup> could be applied to build up a higher fidelity resource than can be achieved by direct transmission. This can then be used to transfer quantum states or some form of quantum communication. In effect, the concept of a quantum repeater<sup>23</sup> could be employed in a solid state, spin chain scenario.

It is clear from the oscillatory behaviour of the dynamics that branched spin chain systems could be operated “in reverse”, for example providing a method of detecting certain entangled states. If an entangled state is fed into the ends of branches it can deliver a signature at a certain single node or spin (such as the one we have used as the input node in our entanglement creation scenarios). This could be detected with just a single-qubit measurement. In more involved scenarios, entangled states could also be prepared non-locally, through a simple conditioning measurement on one or more spins, in conjunction with the natural spin chain dynamics acting on some simple initial state.

Finally, we comment that all these related effects result from the basic dynamics of the branched spin chain systems and simply prepared initial states. Whilst some control is need over the couplings to achieve entanglement creation, distribution and isolation, there is certainly significant potential for branched spin chain systems in solid state quantum processing and communication. This potential will continue to grow, as fabrication or creation of solid state systems that can operate as spin chains continues to progress.

BWL acknowledges support from the Royal Society through a University Research Fellowship, the QIPIRC ([www.qipirc.org](http://www.qipirc.org), GR/S82176/01), DSTL and St Anne’s College, Oxford. IDA acknowledges support from the Dept. of Physics, University of York, and the kind hospitality of Hewlett Packard Labs, Bristol, and the Department of Ma-

terials, University of Oxford.

---

<sup>\*</sup> Electronic address: ida500@york.ac.uk  
<sup>†</sup> Electronic address: brendon.lovett@materials.oxford.ac.uk  
<sup>‡</sup> Electronic address: tim.spiller@hp.com

<sup>1</sup> N. Gisin, G. Ribordy, W. Tittel and H. Zbinden, *Rev. Mod. Phys.* **74**, 145, (2002).  
<sup>2</sup> S. Bose, *Phys. Rev. Lett.* **91**, 207901, (2003).  
<sup>3</sup> T. J. Osborne and N. Linden, *Phys. Rev. A* **69**, 052315, (2004).  
<sup>4</sup> M. Christandl, N. Datta, A. Ekert and A. J. Landahl, *Phys. Rev. Lett.* **92**, 187902 (2004).  
<sup>5</sup> M. Christandl, N. Datta, A. C. Dorlas, A. Ekert, A. Kay, A. J. Landahl, *Phys. Rev. A* **71**, 032312 (2005).  
<sup>6</sup> G. De Chiara, D. Rossini, S. Montangero and R. Fazio, *Phys. Rev. A* **72**, 012323 (2005).  
<sup>7</sup> M.-H. Yung and S. Bose, *Phys. Rev. A* **71**, 032310 (2005).  
<sup>8</sup> D. Burgarth and S. Bose, *Phys. Rev. A* **71**, 052315 (2005).  
<sup>9</sup> D. Burgarth and S. Bose, *New J. Phys.* **7**, 135 (2005).  
<sup>10</sup> A. Wojcik, T. Luczak, P. Kurzynski, A. Grudka, T. Gdala and M. Bednarska, *Phys. Rev. A* **72**, 034303, (2005).  
<sup>11</sup> I. D'Amico, "Relatively short spin chains as building blocks for an all-quantum dot quantum computer architecture" in 'Focus on Semiconductor Research' (2006) (edited by Nova Science Publishers), cond-mat/0511470.  
<sup>12</sup> M. B. Plenio and F.L. Semiao, *New J. Phys.* **7**, 73 (2005).  
<sup>13</sup> M. J. Hartmann, M. E. Reuter and M. B. Plenio, *New J. Phys.* **8**, 94 (2005).  
<sup>14</sup> M. Avellino, A. J. Fisher and S. Bose, *Phys. Rev. A* **74**, 012321 (2006).  
<sup>15</sup> A. D. Greentree, S. J. Devitt and L. C. L. Hollenberg, *Phys. Rev. A* **73**, 032319 (2006).  
<sup>16</sup> T. Ohshima, A. Ekert, D. K. L. Oi, D. Kaslizowski and L. C. Kwek, "Robust state transfer and rotation through a spin chain via dark passage", quant-ph/0702019.  
<sup>17</sup> S. J. Devitt, A. D. Greentree and L. C. L. Hollenberg, "Information free quantum bus for universal quantum computation", quant-ph/0511084.  
<sup>18</sup> M. Paternostro, H. McAneney and M. S. Kim, *Phys. Rev. Lett.* **94**, 070501 (2005).  
<sup>19</sup> T. P. Spiller, I. D'Amico and B. W. Lovett, *New J. Phys.* **9**, 20 (2007).  
<sup>20</sup> C. H. Bennett, G. Brassard, C. Crepeau, R. Jozsa, A. Peres and W. Wootters, *Phys. Rev. Lett.* **70**, 1895 (1993).  
<sup>21</sup> C. H. Bennett, G. Brassard, S. Popescu, B. Schumacher, J. A. Smolin, and W. K. Wootters, *Phys. Rev. Lett.* **76**, 722 (1996).  
<sup>22</sup> W. J. Munro, D. F. V. James, A. G. White and P. G. Kwiat, *Phys. Rev. A* **64**, 030302 (2001)  
<sup>23</sup> H.-J. Briegel, W. Dür, J. I Cirac and P. Zoller, *Phys. Rev. Lett.* **81**, 5932 (1998).